ELSEVIER

Journal of Power Sources 68 (1997) 195–200

JOURNAL OF POWER SOURCES

Pyrolysed silicon-containing polymers as high capacity anodes for lithium-ion batteries

A.M. Wilson [a], G. Zank [b], K. Eguchi [b], W. Xing [a,1], J.R. Dahn [a,*,2]

[a] *Department of Physics, Simon Fraser University, Burnaby, BC, V5A 1S6 Canada*

[b] *Dow–Corning Asia Ltd., Yamakita, Kanagawa 258–01, Japan*

Accepted 2 October 1996

Abstract

We describe the characteristics of materials prepared by the pyrolysis of over 50 different silicon-containing polymers, including polysilanes, polysiloxanes, and pitch silane blends. We investigate the electrochemical behaviour and structural properties of these materials as a function of their stoichiometry. Based on our findings we propose a structural phase diagram which illustrates possible structures of these materials. Our results suggest that the electrochemical behaviour of these materials, as might be expected, varies with stoichiometry and structure. We recommend stoichiometric ranges to be avoided for lithium-ion battery applications. © 1997 Published by Elsevier Science S.A.

Keywords: Lithium-ion batteries; Silicon polymers; Anodes

1. Introduction

In order to improve the performance and decrease the size of Li-ion batteries, it is necessary to increase the specific capacity and volumetric energy density of both the anode and the cathode materials.

In the past, we have increased the capacity of carbonaceous Li-ion battery anodes by preparing carbonaceous materials which contain silicon or silicon and oxygen [1–4]. Here we investigate silicon oxycarbide glasses of varying stoichiometry and structure, made by pyrolysing silane-pitch blends, polysilanes, and polysiloxanes.

Polysilanes and polysiloxanes are commonly used to make silicon carbide [5,6]. By heating to lower temperatures and using different precursors, we have made silicon oxycarbides (Si–O–C), which retain most of the oxygen in the precursor. The X-ray powder diffraction profile and electrochemical behaviour of some Si–O–C is presented. Many of these materials are almost amorphous and have large capacities.

A Gibbs triangle is used to map the weight percentages of C, Si, and O in the final ceramic. Because of the confined range of stoichiometries we are investigating, for reasons of simplicity in this study, a portion of the entire triangle is used. Fig. 1 shows the subset of the entire range of stoichiometries chosen. The corners are C, SiC, and SiO_2. Here, SiC and SiO_2 represent materials with the average stoichiometries indicated, but are not necessarily crystalline SiC or SiO_2.

2. Experimental

Highly cross-linked polysilanes and polysiloxanes were synthesized at Dow–Corning. The pitch-silane derivatives were prepared by blending, at various weight ratios, an Ashland Chemical pitch with a polysilane. The polysilanes were prepared from the sodium coupling of mixtures of chlorosilanes.

Polymer and blend pyrolysis took place under constant flushing with ultra-high purity argon (Linde, 99.999%) gas. The flush rate maintained was sufficient to prevent the decomposition and redeposition of vapours released during polymer decomposition. The samples were placed in the reaction tube at 100 °C and flushed with a volume of argon sufficient to fill the reaction tube 20 times. The temperature was raised at a rate of 5 °C/min to the maximum temperature. The maximum temperature was maintained for 60 min. Most samples discussed here, unless otherwise stated, were pyrolysed at a

* Corresponding author.

[1] Permanent address: Department of Physics, Dalhousie University, Halifax, NS, B3H 3J5 Canada

[2] Permanent address: Department of Physics, Dalhousie University, Halifax, NS, B3H 3J5 Canada.

PII S0378-7753(96)02551-7

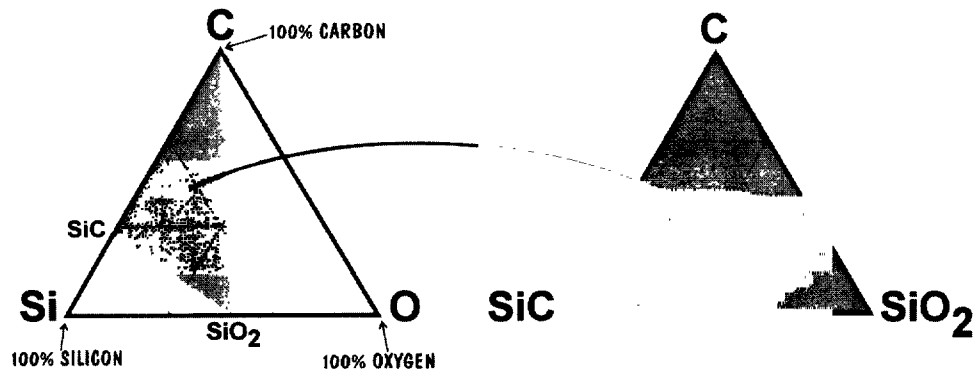

Fig. 1. The Gibbs triangle used to map the stoichiometry (in wt.%). The shaded triangle on the left represents the subset investigated and is enlarged as the equilateral triangle on the right.

Table 1
Summary of the samples (PB: pitch blend, SP synthetic polysiloxanes)

Sample ID	Precursor	Reversible capacity (mAh/g)	Irreversible capacity (mAh/g)	Average charge voltage (V)	Average discahrge voltage (V)
A	PB	543	138	0.67	0.34
B	SP	364	240	0.77	0.30
C	SP	340	188	0.72	0.30
D	SP	191	476	0.86	0.14
E	SP	706	297	0.83	0 33
F	SP	920	308	1.08	0.34
G	PB	520	180	0.74	0.35
H	PB	470	210	0.80	0.34
I	PB	340	200	0.77	0.36
J	PB	350	150	0.76	0 35
K	Pitch	360	70	0.60	0 25
L	PB	60	290	1.10	0.15
M	PB	620	360	1.17	0.37
N	PB	500	160	0.68	0.34

maximum temperature of 1000 °C. Cooling to 100 °C was at a rate of approximately 4 °C/min.

Samples B, C, D, E, and F were synthetic polymers pyrolysed at a maximum temperature of 1000 °C. Samples G, A, H, I, and J were pitch blends (pyrolysed at a maximum temperature of 1000 °C). Sample K is Ashland pitch pyrolysed at a maximum temperature of 1000 °C. Samples L, M, and N were made by heating the sample G precursor at maximum pyrolysis temperatures of 600, 800, and 1100 °C, respectively.

Elemental analysis of the resulting materials was performed at Dow–Corning Corporation. We used a Siemens D5000 diffractometer to perform X-ray diffraction, as described elsewhere [1–4].

For test purposes, all samples were used as cathodes in cells opposite 125 μm Li foil anodes. The details of cell construction have been explained elsewhere [7]. The electrolyte used was 1 M $LiPF_6$ dissolved in a 70/30 vol.% (v/o) mixture of ethylene carbonate and diethyl carbonate. All cells were cycled using a constant current of 18.6 mA/g.

3. Results and discussion

Of the materials studied we are presenting 14, as summarized in Table 1. Fig. 2 shows the stoichiometry (closed on elemental analysis of the ceramic) of many of the samples made, with samples A through G labeled.

Fig. 3 shows the powder X-ray diffraction and voltage profiles for samples A through G. Samples A, E, F, and G have diffraction profiles similar to that of a disordered carbon. The 43° peak is caused by the honeycomb structure of small graphene sheets, showing that at least some carbon is present in an $(sp)^2$ bonded configuration. The broad peak around 25° shows that there is little parallel stacking of the graphene sheets. Considering their stoichiometry, there are obviously

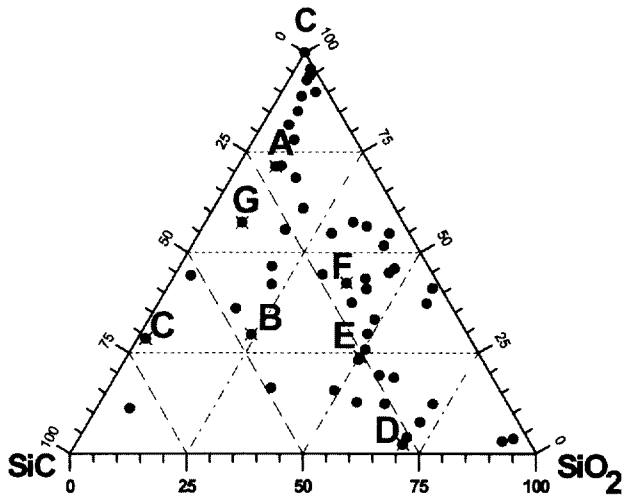

Fig. 2. Gibbs triangle showing the stoichiometry of many samples to date. Samples A through G are labeled.

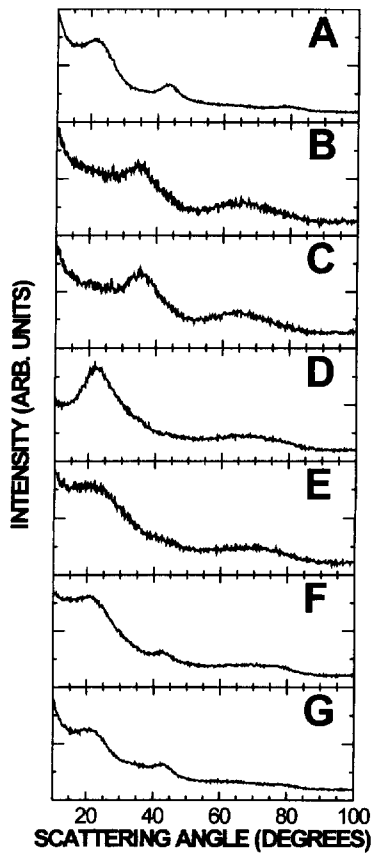

Fig. 3. Diffraction profiles for samples A to G.

other constituents in the material which must be amorphous, and thus not visible in the X-ray diffraction profiles. Samples A and G show little hysteresis (the difference between charge and discharge voltages). They have voltage profiles like an extended capacity coke, similar to the CVD materials made by Wilson et al. [1,2]. For samples E and F, there is a greater difference between the charge and discharge voltages.

The powder diffraction profiles of samples B and C (Fig. 3) show very broad peaks, identified as amorphous or small particle SiC. We believe that B is an intimately mixed composite of very small SiC grains with oxycarbide glass. Sample C is believed to be SiC with some excess carbon substituting at some silicon sites. The voltage profiles (Fig. 4) show poor performance, since SiC does not react with Li.

The powder diffraction profile for sample D (Fig. 3) is similar to that of a-SiO_2, indicating it is a networked glass-containing carbon. This material exhibits a large irreversible and a small reversible capacity.

The voltage profiles (Fig. 4), especially E and F, show that Li is removed from these materials at notably higher voltages than it was inserted. The powder diffraction profiles for E and F show evidence for oxycarbide glass and disordered carbon, whereas the A and G profiles show only disordered carbon. The difference in average voltage between charge and discharge decreases with diminishing evidence for the oxycarbide glass structure (from 0.98 V for sample E to 0.39 V for sample G). Samples which have less of a glass structure and more of a disordered carbon structure exhibit less of a voltage difference between charge and discharge.

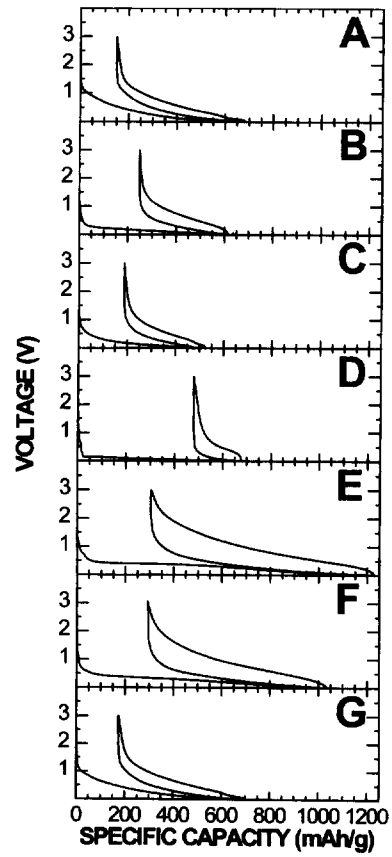

Fig. 4. Voltage profiles for samples A to G.

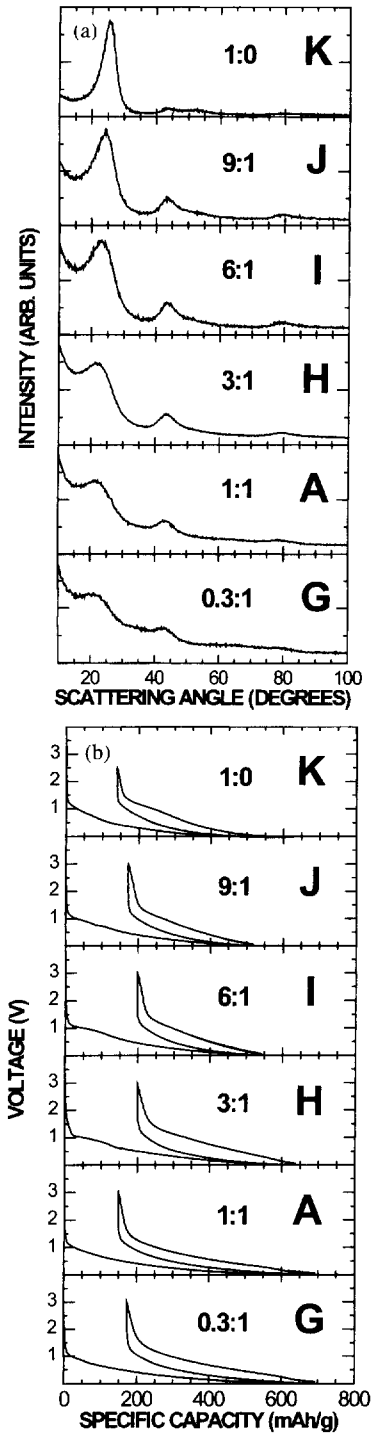

Fig 5 (a) Powder diffraction profiles; (b) voltage profiles for various pitch to silane blend ratios.

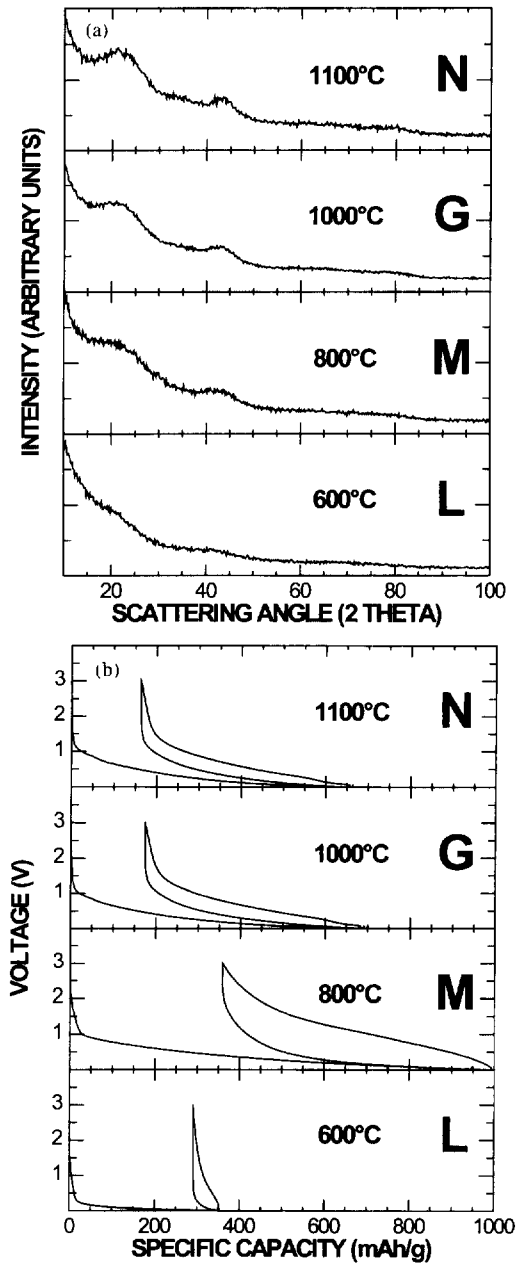

Fig 6. (a) Powder diffraction profiles; (b) voltage profiles for 0.33:1 pitch to silane blend at various maximum pyrolysis temperatures

Samples G, A, H, I, J, and K are all pitch blends pyrolysed at 1000 °C with pitch to polysilane ratios of 0.33:1, 1:1, 3:1, 6:1, 9:1, and 1:0, respectively. The powder diffraction and voltage profiles are shown in Fig. 5 in order of least (top) to most (bottom) silane. As the amount of polysilane in the precursor increases the disorder in the pyrolysed material increases. The 25° peak shows a more pronounced decrease in intensity than the 43° peak. Thus, the silane is interfering more with the layer stacking than the lateral extent of the layers. The voltage profiles (Fig. 5(b)), show that the capacity increases roughly with the silane concentration in the precursor.

Samples L, M, G, and N are the same blend of pitch:polysilane (ratio 0.33:1) heated to 600, 800, 1000, and 1100 °C, respectively. The powder diffraction profile (Fig. 6(a)) shows that at 600 °C the material has almost no order, whereas at higher temperatures more order is observed.

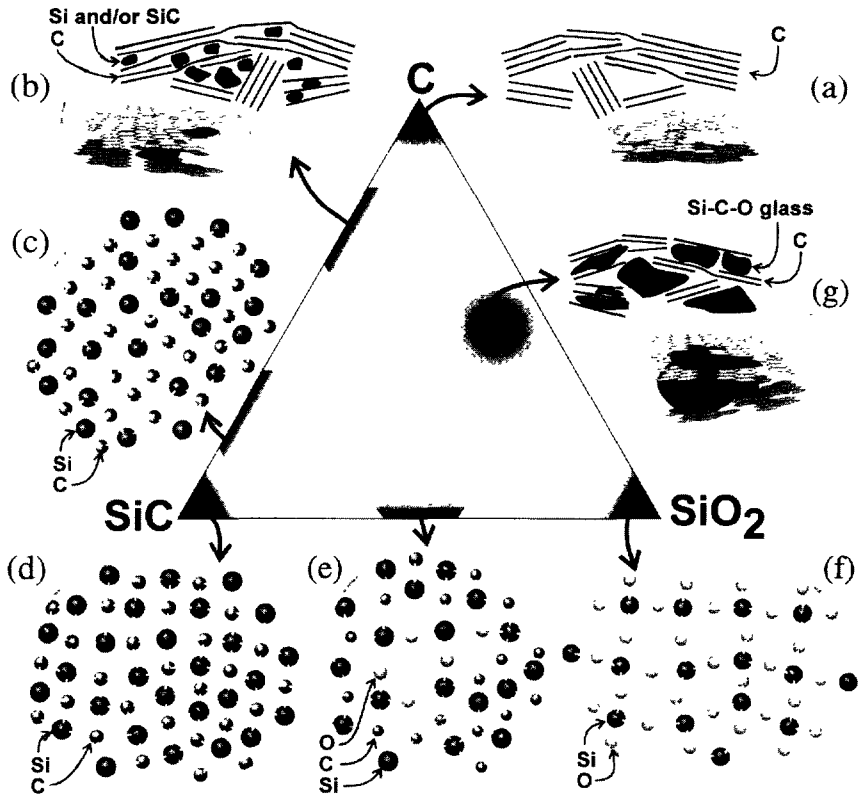

Fig. 7. Structural schematic phase diagram for the materials presented here The structures presented should be treated as an artists conception of possible structures

The poorly developed 25° peak shows that there is very little parallel stacking of graphene layers. The 43° peak shows that the lateral extent of the layers increases from 600 to 1100 °C. The voltage profile of the material treated at 600 °C shows almost no capacity, due to poor conductivity. The voltage profile of the 800 °C material shows behaviour indicative of Li bonding to a C atom which is also bonded to H [8]. By 1000 °C, most of the H has been removed and the material shows little difference between charge and discharge voltages, while the capacity is much larger than a typical pitch heated in this manner.

4. Conclusions

Based on our findings, we have constructed a structural phase diagram, for our series of materials. Shown in Fig. 7, it is important to stress that this is a schematic, and should be treated as an artists' conception of possible structures. Fig. 7(a) shows a typical disordered carbon, with stacking faults, turbostratic disorder, and graphene sheet defects. Fig. 7(b) shows materials containing nanodispersed silicon, silicon carbide, or both. Fig. 7(c) shows SiC with additional C substituting in some of the Si sites. It is believed that once there is sufficient carbon, it will be more energetically favourable to form areas of disordered carbon ($(sp)^2$ bonded), rather than forming further diamond-like (sp^3) bonds. Fig. 7(d) and (f) shows amorphous SiC and SiO_2, respectively. Fig. 7(e) shows a possible transition material, between SiC and SiO_2. Fig. 7(g) shows a material similar to that shown in Fig. 7(b), although here the material located between the carbon regions is a silicon oxycarbide glass.

Samples B, C, and D show that the extremes near the SiC and SiO_2 corners of the triangle should be avoided. In these regions, SiC and SiO_2 are likely to form, contributing 'dead weight' to the battery. Si–O–C's represent an interesting range of materials, both for study and industrial applications. However, the nature of the Li insertion needs to be understood in order to attempt reduction of the irreversible reaction and the charge to discharge voltage difference.

References

[1] A.M. Wilson and J.R. Dahn, *J. Electrochem. Soc.*, *142* (1995) 326–332

[2] A.M. Wilson, B.M. Way, J.R. Dahn and T. van Buuren, *J. Appl Phys.*, *77* (1995) 2363

[3] A.M. Wilson, J N. Reimers, E. Fuller and J.R. Dahn, *Solid State Ionics, 74* (1994) 249–254.
[4] J.S. Xue, K. Myrtle and J.R. Dahn, *J. Electrochem. Soc., 142* (1995) 2927–2935
[5] G.T. Burns, R B. Taylor, Y. Xu, A. Zangvil and G.A. Zank, *Chem. Mater., 4* (1992) 1313–1323.
[6] M.A. Abu-eid, R B. King and A.M. Kotliar, *Eur. Polym J., 28* (1992) 315–320.
[7] W. Xing, J S Xue and J.R. Dahn, *J Electrochem. Soc., 143* (1996) 3046.
[8] T. Zheng, J.S. Xue and J.R Dahn, *Chem Mater., 8* (1996) 389–393.